Direct synthesis of water-dispersible 2 nm FePt nanocrystals without ligand exchange

HongLing Liu [a,*], XiaoYan Zhang [a], Peng Hou [a], JunHua Wu [b,*]

[a] Institute of Molecular and Crystal Engineering, School of Chemistry and Chemical Engineering, Henan University, Kaifeng 475004, China
[b] Pioneer Research Center for Biomedical Nanocrystals, Korea University, Seoul 136-713, Republic of Korea

ABSTRACT

Water-dispersible 2 nm FePt ultrasmall nanocrystals coated by a biocompatible triblock copolymer, poly(ethylene glycol)-block-poly(propylene glycol)-block-poly(ethylene glycol) (PEO-PPO-PEO) were directly synthesized in a single-step nanoemulsion process. The FTIR investigation proves the PEO-PPO-PEO molecules on the surface of the resulting nanocrystals, which render the nanocrystals hydrophilic for aqueous dispersion without using conventional ligand exchange and offer proper protection of the nanocrystals from oxidation. The structural and morphological analysis reveals both single-crystallinity and high crystallinity of the nanocrystals in the face-centered cubic phase, with an excellent monosize distribution of 1.95 ± 0.18 nm in diameter. Moreover, the polymer-capped nanocrystals possess well-defined magnetic behavior and the aqueous dispersion–collection process of the nanocrystals was demonstrated for application readiness of such ultrasmall nanocrystals in aqueous media.

1. Introduction

The iron–platinum (FePt) binary metallic alloy nanostructures, owing to the extraordinary high magnetocrystalline anisotropy constant in the bulk phase ($K_u = 7 \times 10^7$ erg cm^{-3}) and other excellent physicochemical properties of the material, have been investigated for various applications, including high-density magnetic memory storage media, biomedical imaging and sensing, magnetic separations, and catalysis [1–13]. In the research, diverse methods have been proposed to synthesize FePt nanoparticles, for which toxic precursors were often employed [11–24]. Of great interest is the preparation of exceptionally small FePt nanoparticles, particularly near the critical dimension of ~2 nm in diameter. Currently obtained in a superparamagnetic state under the ambient condition, such nanoparticles could be made pertinent in exploring potential high density magnetic recording media through proper nanoengineering and for biomedical uses in which the physicochemical and pharmacokinetic properties are affected sensitively by the particle size. For a miniature particle size, however, spontaneous oxidation and finite-size effects could turn out to be a serious issue challenging the perspective applications of FePt nanoparticles, demanding extra protection to avoid deterioration of their magnetic properties [25–27]. Presently, proper surface tailoring is exercised to provide an attractive and effective approach for the

protection functioning. In addition, a biofriendly, functionalizable surface is actively sought for biomedical purposes, usually acquired through a second step of surface modification [28,29]. The solution to the issues raised above has generated encouraging success, but a more effective, easy tactic is greatly appreciated and continues to be pursued.

We have focused on preparing a variety of nanoparticles by means of nanoemulsion methodologies, particularly using polymer surfactants including poly(ethylene glycol)-block-poly(propylene glycol)-block-poly(ethylene glycol) (PEO-PPO-PEO) and poly(vinylpyrrolidone) (PVP) [30–33]. The PEO-PPO-PEO triblock copolymer and related polymer families have many extraordinary merits such as aqueous solubility, non-charging, non-toxicity, and are frequently used in a number of fields [30–32,34–37]. In the nanoemulsion processes, the PEO-PPO-PEO molecules principally participate in the reactions as a surfactant and form a thin coating on the resultant nanoparticles to stabilize and protect them from oxidation [30–32]. On the basis of our precedent research that has produced long-term stable, highly crystalline, monosized AuFe and Fe$_3$O$_4$/Au core–shell nanoparticles applying the PEO-PPO-PEO surfactant for biomedical applications [30–32], we report in this work the direct synthesis and characterization of water-dispersible ultrasmall FePt nanocrystals by one-step nonaqueous nanoemulsion assisted by PEO-PPO-PEO, but without using ligand exchange for aqueous dispersion of the nanocrystals. Meanwhile, non-toxic precursors were used in the process, instead of toxic iron carbonyl (Fe(CO)$_5$). The FePt nanocrystals as synthesized were analyzed by Fourier transform

* Corresponding authors. Tel.: +82 2 3290 3899.
  E-mail addresses: hlliu@henu.edu.cn (H. Liu), feitianshenhu@yahoo.com (J. Wu).

infrared spectroscopy (FTIR), transmission electron microscopy (TEM) including high resolution imaging (HRTEM), powder X-ray diffraction (XRD), vibrating sample magnetometry (VSM)/Physical Property Measurement System (PPMS) and UV–visible spectroscopy (UV–vis).

2. Experimental

2.1. Materials

The two precursors used for the nanoemulsion synthesis of the PEO-PPO-PEO-coated FePt nanocrystals were platinum acetylacetonate (Pt(acac)$_2$, 99.99%) and iron (II) acetylacetonate (Fe(acac)$_2$, 99.95%). The PEO-PPO-PEO triblock copolymer (M_n = 5800) was utilized as the surfactant, with 1,2-hexadecanediol (C$_{14}$H$_{29}$CH(OH)CH$_2$(OH), 90%) as the reducing agent. Other chemicals included octyl ether (C$_8$H$_{17}$OC$_8$H$_{17}$, 99%) and solvents such as hexane and ethanol. All materials were purchased from Aldrich and were used as received.

2.2. Synthesis of polymer-coated FePt nanocrystals

The synthesis of the PEO-PPO-PEO-coated FePt ultrasmall nanocrystals with a nominal ratio of 1:1 was carried out as follows. In a typical experiment, 0.25 mmol Fe(acac)$_2$ in 10 ml dioctyl ether was mingled with 0.25 mmol Pt(acac)$_2$, the reduction agent of 1,2-hexadecanediol (2.5 mmol) and the PEO-PPO-PEO surfactant in a 250 ml flask. Under vigorous stirring, the reaction mixture was first heated to 80 °C and homogenized at the temperature for 1 h, then rapidly raised to 280 °C and refluxed at the temperature for 1 h to complete the reaction. Subsequently, ethanol was added to the reacted mixture to precipitate the nanocrystals after cooling down to room temperature. The resulting black product was separated from the supernatant by centrifugation and washed with the mixed solvents of ethanol/hexane (1:2) twice and re-dispersed in hexane. For a comparative investigation, similar syntheses were performed using either Fe(acac)$_2$ or Pt(acac)$_2$ only to prepare the corresponding nanocrystals.

2.3. Characterization and analysis of polymer-coated FePt nanocrystals

The polymer coating on the nanocrystals was examined by FTIR. In the measurement, the washed FePt nanocrystals and the pure PEO-PPO-PEO polymer were crushed with a pestle in an agate mortar, separately. The individually crushed material was then mixed with potassium bromide (IR spectroscopy grade, Merck, Germany) in the proportion of ∼1:100. Subsequently, the mixture was compressed into a 2 mm semi-transparent disk by applying a force of 10 tons for 2 min. The FTIR spectra were recorded in the range of 4000–400 cm^{-1} using an Avatar 360 FTIR spectrometer (Nicolet Company, USA). The morphology, particle size and size distribution of the PEO-PPO-PEO-coated FePt ultrasmall nanocrystals were analyzed by TEM (JEM-100II and JEOL 2010F) including HRTEM, whereas the crystal structure of the nanocrystals was studied by XRD (X'Pert Pro). In addition, magnetic measurements were performed on the dried samples by VSM (Lakeshore 7300) and PPMS (Quantum Design) to evaluate the magnetic properties of the nanocrystals over a broad range of temperature. The absorption properties of the samples were characterized by UV–vis (Hitachi U4100).
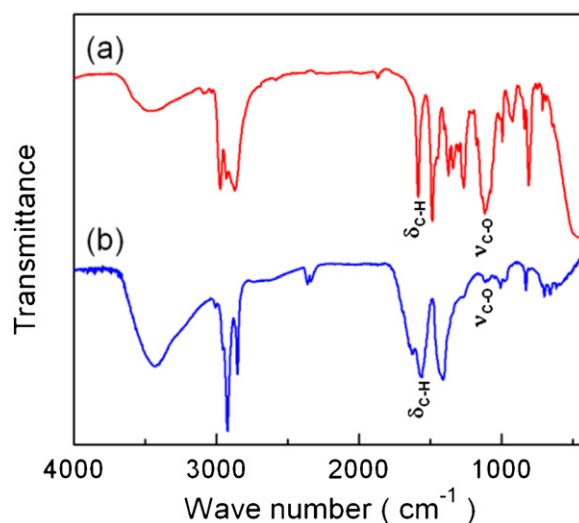

Fig. 1. FTIR spectra of (a) the pure PEO-PPO-PEO molecules and (b) the PEO-PPO-PEO-coated FePt nanocrystals. The ν_{C-O} and δ_{C-H} bands are indicated.

3. Results and discussion

The PEO-PPO-PEO-coated FePt ultrasmall nanocrystals with a nominal ratio of 1:1 were obtained by simultaneous thermal reduction of Fe(acac)$_2$ and Pt(acac)$_2$ by 1,2-hexadecanediol in the nano-micelles (nanoreactors) formed by the PEO-PPO-PEO macro-molecules. The covering of the polymer molecules on the surface of the FePt nanocrystals was comparatively examined by FTIR on both the purified nanocrystals and the pure polymer itself [31]. Fig. 1 shows the FTIR spectrum of the FePt nanocrystals after purification against that of the same PEO-PPO-PEO molecules used in the nanoemulsion. In Fig. 1a, the pure PEO-PPO-PEO molecules show one strong characteristic band at the position of ∼1120.5 cm^{-1} for the C–O–C stretching vibration of the ether bonding and one sharp characteristic band for the C–H bending vibration at the position of ∼1587.2 cm^{-1} [31,34]. In contrast, the position of the C–O–C stretching vibration, as shown in Fig. 1b, changes slightly to ∼1114.7 cm^{-1} in the FTIR spectrum of the FePt nanocrystals, but the absorption intensity diminishes tremendously. In the meantime, the original characteristic C–H bending band shifts to the position of 1569.8 cm^{-1} with a shoulder at 1629.6 cm^{-1} in the FePt nanocrystals. Considerably different from the pure PEO-PPO-PEO molecules to the PEO-PPO-PEO-coated FePt nanocrystals, the shifting in the band positions and the change in the band shapes of the C–O–C stretching and C–H bending bands may engage the coordination of the oxygen atoms in the main chains with the Pt metallic atoms and as a result of straining of the bonds on the small surface of high curvature [38,39]. Since the redundant PEO-PPO-PEO molecules were removed by the purification procedure, the observation in Fig. 1 explicitly highlights the coating of the PEO-PPO-PEO molecules onto the surface of the FePt nanocrystals, which are further consolidated by the other relevant absorption bands in the spectra. As demonstrated below, the hydrophilic surface of the FePt nanocrystals owing to the PEO-PPO-PEO-capping enables an easy transfer of the nanocrystals to an aqueous medium without more surface decoration or a secondary ligand exchange, leading to readiness for biomedical applications which generally require proceeding in an aqueous medium. Conversely, a second step of surface modification is commonly involved for similar nanoparticles to become water dispersible from other routes such as using oleic acid and/or oleylamine as the capping agent, as a consequence of formation of the hydrophobic surface [28,29].
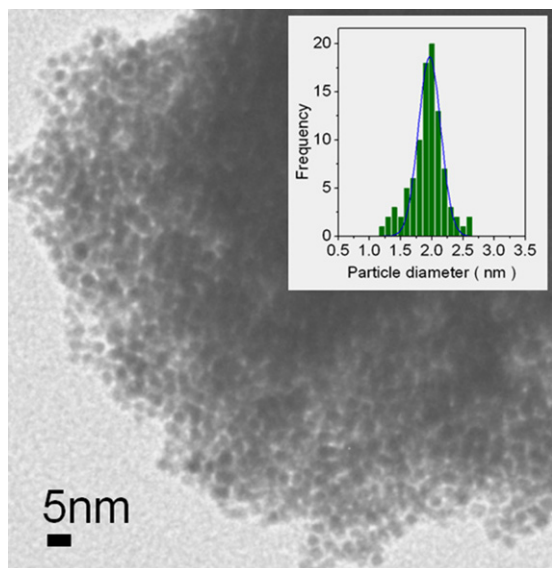
Fig. 2. Bright-field TEM image of the FePt nanocrystal assembly. Inset: particle size histogram and its Gaussian fit.
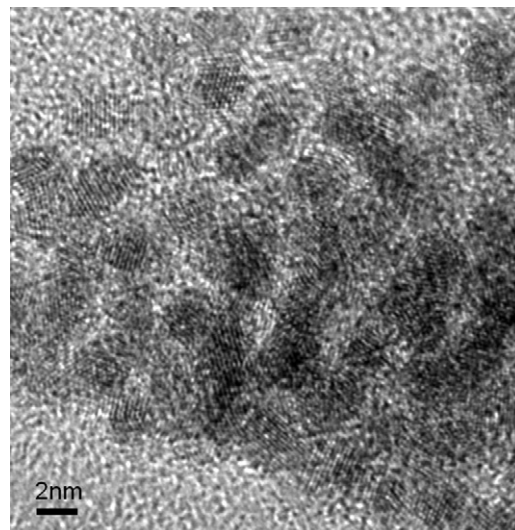

Fig. 3. HRTEM image of the PEO-PPO-PEO-capped FePt ultrasmall nanocrystal assembly.
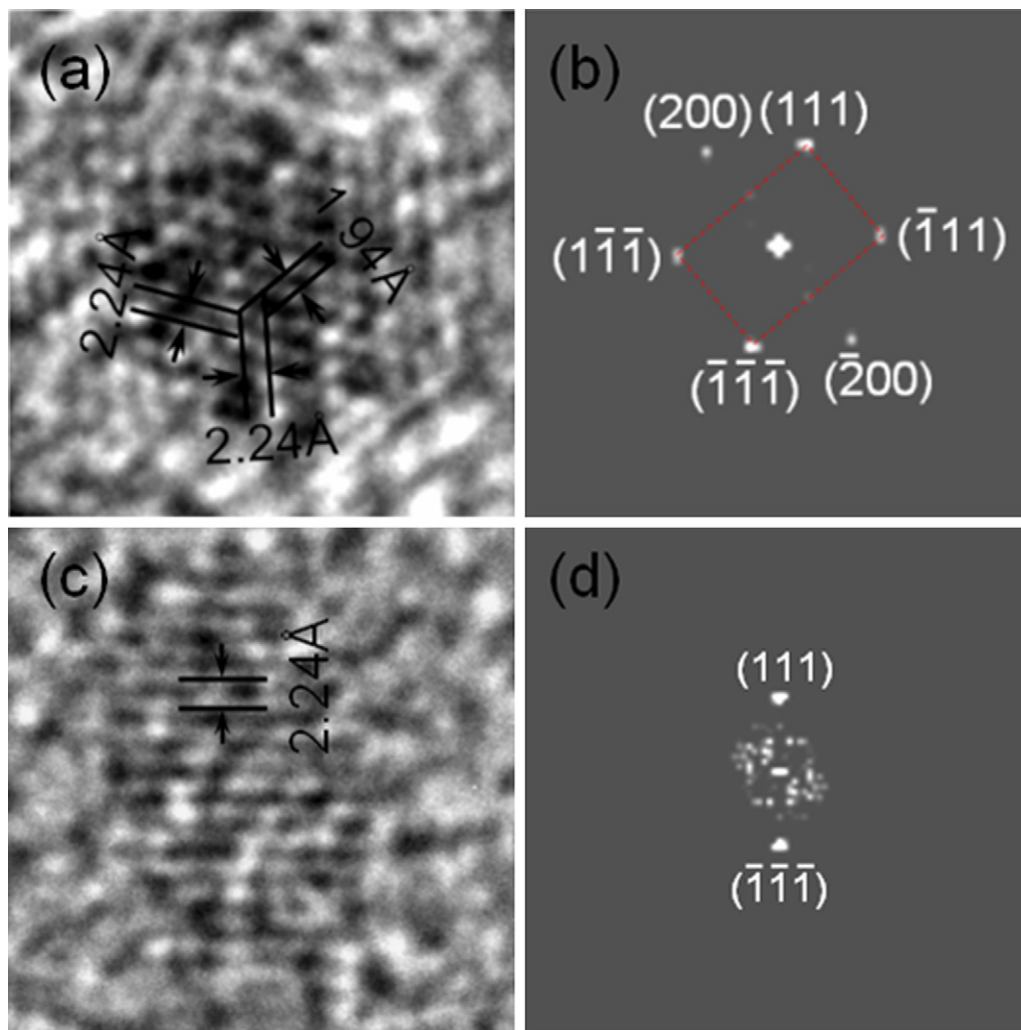

Fig. 4. HRTEM analysis of two representative single-crystalline PEO-PPO-PEO-capped FePt ultrasmall nanocrystals. (a and b) Lattice image and its FFT transform with the indexing of the projected atomic columns in the roughly rounded nanocrystal. The spacings of 2.24 Å and 1.94 Å correspond to the fcc FePt (1 1 1) and (2 0 0) reflections. (c and d) Lattice image and its FFT transform with the labelling of the projected atomic columns in the elongated nanocrystal. The spacing of 2.24 Å corresponds to the fcc FePt (1 1 1) reflection.
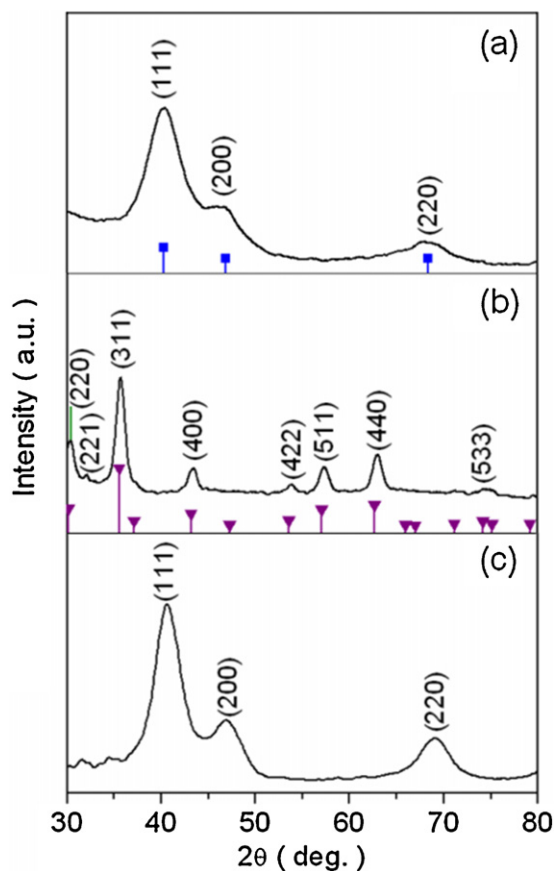
Fig. 5. XRD analyses of relevant nanocrystals prepared the same way. (a) Pattern of the ultrasmall FePt nanocrystals. Bar diagram for JCPDS of fcc FePt. (b) Pattern of Fe_3O_4 nanocrystals from $Fe(acac)_2$. (2 2 1) is an anomalous Fe_3O_4 reflection. Bar diagram for Fe_3O_4 JCPDS. (c) Pattern of Pt nanocrystals from $Pt(acac)_2$.

Fig. 2 shows the morphology and particle sizes of the PEO-PPO-PEO-coated FePt nanocrystals recorded by TEM. Obviuosly, the nanocrystals are extremely small and almost uniform, revealing the behavior of self-assembling. The particle size distribution of the nanocrystals, as shown in the inset, is statistically monosized obeying a Gaussian fit and gives an average particle size of 1.95 ± 0.18 nm in diameter, indicating an excellent monodispersity of ~9%. Referring to the crystallographic parameter obtained from the lattice images and the diffraction analysis in the next sections, the nanocrystals have an averaged dimension equivalent to five unit cells, which is critically small but still reveal well-behaved magnetic properties as justified later [2,27]. Thus, the present nanoemulsion method efficiently affords an alternative process to prepare 2 nm FePt nanocrystals protected by the biocompatible polymer molecules.

The crystal structure and microstructural details of the ultrasmall PEO-PPO-PEO capped FePt nanocrystals were elucidated by both HRTEM imaging and XRD analysis. Fig. 3 gives an overview of the nanocrystals across a large area, demonstrating the highly crystalline nature of the nanocrystals as evidenced by the omnipresence of the distinct lattices from the projection of the atomic columns. The FePt nanocrystals are obviously oriented randomly, consistent with the outcome of the selected-area electron diffraction (SAED) which shows a powder pattern as a result of the superimposed diffractions of the disoriented nanocrystals. Fig. 4 zooms in on two representative FePt nanocrystals, exploiting the fine construction of the corresponding atomic arrangement. Evidently, the fringe lattices of Fig. 4a in two-dimension run almost uniformly over the entire nanocrystal, indicative of the single-crystallinity or
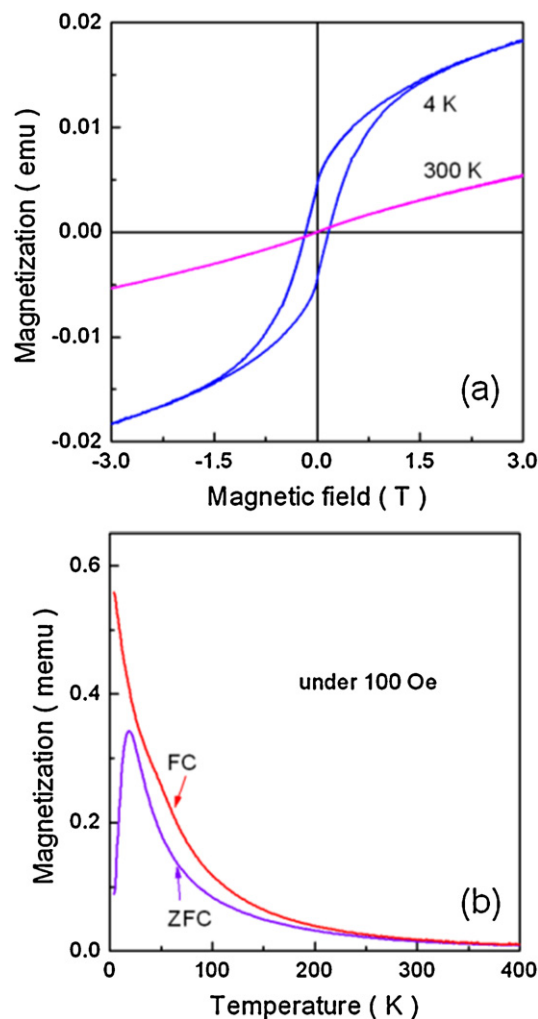

Fig. 6. Magnetic properties of the polymer-coated FePt ultrasmall nanocrystals. (a) Hysteresis curves obtained at 4 K and room temperature, separately. (b) Temperature dependence of the magnetization for the field cooled and zero field cooled under a magnetic field of 100 Oe.

monocrystallinity of the nanocrystal. In the image indexed are the representative lattice spacings of 2.24 Å and 1.94 Å, corresponding to the (1 1 1) and (2 0 0) reflections of the FePt face-centered cubic (fcc) phase. The result agrees with the observation of the XRD diffraction as addressed in the next section. As shown in Fig. 4b, the single-crystallinity of the individual nanocrystal is confirmed yet again by the relevant fast Fourier transform (FFT) of the lattice image. Relative to the roughly round shape of the nanocrystal in Fig. 4a, Fig. 4c gives an example of the nanocrystals rarely visible in the elongated form. As labelled in the image, the lattice spacing of 2.24 Å is in match to the (1 1 1) reflection of the FePt fcc phase, which is furthermore supported by its FFT transform in Fig. 4d. In sum, it is remarkable to have attained the high crystallinity and outstanding monocrystallinity in the ultrasmall FePt nanocrystals.

The crystal structure of the ultrasmall FePt nanocrystals is well represented by the XRD pattern, as shown in Fig. 5a. The diffraction peaks positioning at $40.38°$, $46.80°$ and $68.36°$ are properly indexed to the (1 1 1), (2 0 0) and (2 2 0) planes of fcc FePt, with the crystallographic parameter of 3.877 Å (JCPDS no. 29-0717; bar diagram in the figure). Based on the full width at half maximum (FWHM) of the FePt (1 1 1) peak and applying the Scherrer equation, moreover, the average particle size of the nanocrystals is estimated to be ~2.1 nm, supposed that the peak broadening in the XRD pattern is primarily due to the finite-size of the nanoparticles [40]. The appraisal may
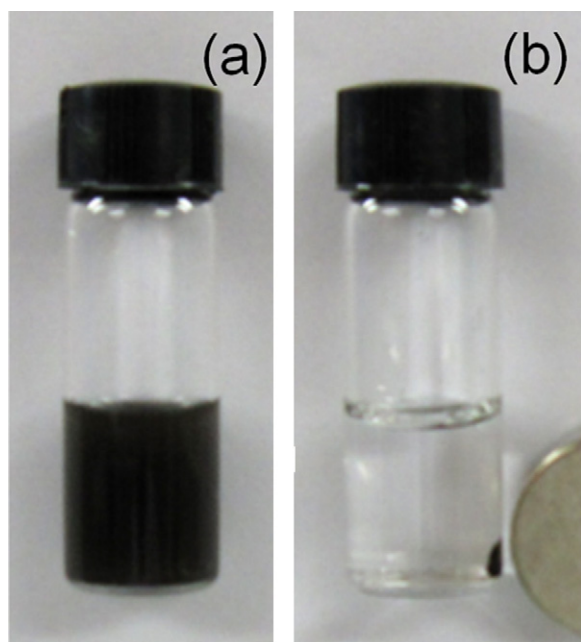
Fig. 7. Photoimages of aqueous dispersion and magnetic manipulation of the polymer-coated FePt ultrasmall nanocrystals. (a) Black, homogeneous dispersion of the nanocrystals in DD water. (b) Clear, transparent solution of the nanocrystals after magnetic separation.

rationally afford supportive evidence with respect to the statistical counting of the TEM analysis above. For a comparison study, similar experiments were conducted using either $Fe(acac)_2$ or $Pt(acac)_2$ alone to synthesize the corresponding nanoparticles, and their XRD diffraction patterns were recorded in Fig. 5b and c, respectively. It is clear that the pattern of the nanocrystals from $Fe(acac)_2$ matches the inverse spinel structure of magnetite (JCPDS no. 19-0629; bar diagram in the figure) and that of the nanocrystals from $Pt(acac)_2$ has an fcc structure of 3.854 Å which is smaller than the value of 3.923 Å of cubic Pt in bulk (JCPDS no. 04-0802). The phenomena present additional convincing corroboration for the formation of the cubic FePt nanocrystals from the simultaneous reduction of $Fe(acac)_2$ and $Pt(acac)_2$. We remark that as there is no evidence of oxidation in terms of the XRD pattern of Fig. 5a, the ultrasmall FePt nanocrystals are well protected by the polymer capping.

In our experiments, according to the XRD analysis and consolidated by TEM, the product of the synthesis results in the FePt nanocrystals which are structurally a single, uniform phase. The composition is FePt, as a result of the starting precursor ratio of $Fe(acac)_2$ to $Pt(acac)_2$ in 1:1, and further corroborated by the TEM-EDX (energy dispersive X-ray analysis) characterization performed on the PEO-PPO-PEO-coated FePt nanocrystals showing the simultaneous presence of both Fe and Pt in the nanoparticle and thus offering direct evidence for the formation of the alloy nanostructure. Consequently, the findings above exclude the possibility of separate Pt and Fe or Fe_3O_4 nanoparticles in the FePt preparation and supports the nanostructuring of the FePt nanocrystals. The outcome is in consistence with other investigations, such as the magnetic analysis as conducted in the following sections.

Furthermore, the magnetic properties of the polymer-coated FePt ultrasmall nanocrystals were studied by VSM and/or PPMS. As shown in Fig. 6a, the hysteresis curves acquired clearly show that the nanocrystals are paramagnetic and/or superparamagnetic at 300 K and become ferromagnetic at 4 K, with a significant enhancement in magnetization as the temperature is lowered. Subsequently, the temperature dependence of the polymer-coated FePt ultrasmall nanocrystals was recorded in an applied magnetic field of 100 Oe in two modes, viz. field cooling (FC) and zero field cooling (ZFC) in the temperature range of 4–400 K (Fig. 6b). As shown in the plots, the nanocrystals manifest the typical superparamagnetic behavior of magnetic nanoparticles, that is, the FC magnetization increases with decreasing temperature, whereas the ZFC magnetization shows different behavior in that it increases initially, reaches a maximum at 18 K (freezing temperature) and then decreases as the sample is further cooled. In contrast, the nanocrystals have a blocking temperature (T_B) estimated to be ~300 K. As usual, the ZFC curve gives a lower value in magnetization than the FC one.

As mentioned above, the ultrasmall FePt nanocrystals could be readily transferred to an aqueous medium without more surface modification or ligand exchange (Fig. 7). Under the influence of an external magnetic field, the nanocrystals experience a change from a black, homogeneous dispersion in double-distilled (DD) water (Fig. 7a) to a clear, transparent solution, with all nanocrystals collected by the magnetic disc (Fig. 7b). The collected nanocrystals can be simply and reversibly dispersed by shaking-up after removing the magnetic field [30,31]. We state that the UV–vis measurements reveal no characteristic absorption band in the visible range for the FePt ultrasmall nanocrystals.

4. Conclusions

We have directly prepared the 2 nm FePt ultrasmall nanocrystals coated by the PEO-PPO-PEO triblock copolymer through the one-pot nanoemulsion synthesis in a single step. The polymer coating renders the nanocrystals hydrophilic, which could be readily transferred into an aqueous medium, and offers proper protection of the nanocrystals from oxidation. The structural and morphological analysis reveals both single-crystallinity and high crystallinity of the nanocrystals in the fcc phase, with an excellent monosize distribution of 1.95 ± 0.18 nm in diameter. Moreover, the polymer-capped nanocrystals show well-defined magnetic behavior, whereas the aqueous dispersion–collection process of the magnetically separable nanocrystals was demonstrated for application readiness of the ultrasmall nanocrystals in an aqueous medium. Such ultrasmall FePt nanocrystals could be interesting in potential high density magnetic recording media and biomedical uses for which the physicochemical and pharmacokinetic properties are affected sensitively by the particle size.

References

[1] D. Weller, A. Moser, L. Folks, M.E. Best, W. Lee, M.F. Toney, M. Schwickert, J.-U. Thiele, M.F. Doerner, IEEE Trans. Magn. 36 (2000) 10–15.
[2] J.-P. Wang, Proc. IEEE 96 (2009) 1847–1863.
[3] L. Toru, K. Yasuo, T. Toshiyuki, A. Mikrajuddin, O. Kikui, J. Appl. Phys. 94 (2003) 6807–6811.
[4] S. Maenosono, T. Suzuki, S. Saita, J. Magn. Magn. Mater. 320 (2008) L79–L83.

[5] H. Yang, J. Zhang, Q. Tian, H. Hu, Y. Fang, H. Wu, S. Yang, J. Magn. Magn. Mater. 322 (2010) 973–977.
[6] J. Gao, H. Gu, B. Xu, Acc. Chem. Res. 42 (2009) 1097–1107.
[7] A. Louie, Chem. Rev. 110 (2010) 3146–3195.
[8] C. Xu, K. Xu, H. Gu, X. Zhong, Z. Guo, R. Zheng, X. Zhang, B. Xu, J. Am. Chem. Soc. 126 (2004) 3392–3393.
[9] S. Shylesh, W.R. Thiel, V. Schunemann, Angew. Chem. Int. Ed. 49 (2010) 3428–3459.
[10] K. Mori, K. Sugihara, Y. Kondo, T. Takeuchi, S. Morimoto, H. Yamashita, J. Phys. Chem. C 112 (2008) 16478–16483.
[11] S. Sun, C.B. Murray, D. Weller, L. Folks, A. Moser, Science 287 (2000) 1989–1992.
[12] J.-L. Tsai, H.-T. Tzeng, G.-B. Lin, Appl. Phys. Lett. 96 (2010), 032505(1–3).
[13] J.-L. Tsai, H.-T. Tzeng, B.-F. Liu, J. Appl. Phys 107 (2010), 113923(1–5).
[14] H.L. Nguyen, L.E.M. Howard, S.R. Giblin, B.K. Tanner, I. Terry, A.K. Hughes, I.M. Ross, A. Serres, H. Burckstummer, J.S.O. Evans, J. Mater. Chem. 15 (2005) 5136–5143.
[15] Y. Gao, X.W. Zhang, Z.G. Yin, S. Qu, J.B. You, N.F. Chen, Nanoscale Res. Lett. 5 (2010) 1–6.
[16] S.N. Shah, N.F. Steinmetz, A.A.A. Aljabali, G.P. Lomonossoff, D.J. Evans, Dalton Trans. (2009) 8479–8480.
[17] K. Liu, C.-L. Ho, S. Aouba, Y.-Q. Zhao, Z.-H. Lu, S. Petrov, N. Coombs, P. Dube, H. Ruda, W.-Y. Wong, I. Manners, Angew. Chem. Int. Ed. 47 (2008) 1255–1259.
[18] V. Monnier, M. Delalande, P. Bayle-Guillemaud, Y. Samson, P. Reiss, Small 4 (2008) 1139–1142.
[19] Q. Yan, A. Purkayastha, T. Kim, R. Kroger, A. Bose, G. Ramanath, Adv. Mater. 18 (2006) 2569–2573.
[20] S.A. Sebt, S.S. Parhizgar, M. Farahmandjou, P. Aberomand, M. Akhavan, J. Supercond. Nov. Magn. 22 (2009) 849–854.
[21] W.S. Seo, S.M. Kim, Y.-M. Kim, X. Sun, H. Dai, Small 4 (2008) 1968–1971.
[22] H. Heller, K. Ahrenstorf, J.A.C. Broekaert, H. Weller, Phys. Chem. Chem. Phys. 11 (2009) 3257–3262.
[23] R.J. Joseyphus, K. Shinoda, Y. Sato, K. Tohji, B. Jeyadevan, J. Mater. Sci. 43 (2008) 2402–2406.
[24] S. Qu, X.-W. Zhang, Z.-G. Yin, J.-B. You, N.-F. Chen, Chin. Phys. Lett. 24 (2007) 3520.
[25] P. de la Presa, T. Rueda, A. Hernando, J.M. Ramallo-Lopez, L.J. Giovanetti, F.G. Requejo, J. Appl. Phys. 103 (2008), 103909(1–8).
[26] L. Han, U. Wiedwald, B. Kuerbanjiang, P. Ziemann, Nanotechnology 20 (2009), 285706(1–7).
[27] T. Iwamoto, K. Matsumoto, T. Matsushita, M. Inokuchi, N. Toshima, J. Colloid Interface Sci. 336 (2009) 879–888.
[28] V. Salgueirino-Maceira, L.M. Liz-Marzan, M. Farle, Langmuir 20 (2004) 6946–6950.
[29] Y. Tanaka, S. Maenosono, J. Magn. Magn. Mater. 320 (2008) L121–L124.
[30] H.L. Liu, C.H. Sonn, J.H. Wu, K.M. Lee, Y.K. Kim, Biomaterials 9 (2008) 4003–4011.
[31] H.L. Liu, P. Hou, W.X. Zhang, Y.K. Kim, J.H. Wu, Nanotechnology 21 (2010), 335602(1–9).
[32] H.L. Liu, J.H. Wu, J.H. Min, J.H. Lee, Y.K. Kim, J. Nanosci. Nanotechnol. 9 (2009) 754–758.
[33] H.L. Liu, P. Hou, W.X. Zhang, J.H. Wu, Colloids Surf. A: Physicochem. Eng. Aspects 356 (2010) 21–27.
[34] T.K. Jain, S.P. Foy, B. Erokwu, S. Dimitrijevic, C.A. Flask, V. Labhasetwar, Biomaterials 30 (2009) 6748–6756.
[35] J. Yang, Y. Zhai, Y. Deng, D. Gu, Q. Li, Q. Wu, Y. Huang, B. Tu, D. Zhao, J. Colloid Interface Sci. 342 (2010) 579–585.
[36] F. Alexis, E. Pridgen, L.K. Molnar, O.C. Farokhzad, Mol. Pharm. 5 (2008) 505–515.
[37] X.-H. Li, D.-H. Zhang, J.-S. Chen, J. Am. Chem. Soc. 128 (2006) 8382–8383.
[38] K. Nakamoto, Infrared and Raman Spectra of Inorganic and Coordination Complexes, Wiley, New York, 1978.
[39] H.L. Liu, J.H. Wu, J.H. Min, P. Hou, A.-Y. Song, Y.K. Kim, Nanotechnology 22 (2011), 055701(1–7).
[40] B.D. Cullity, S.R. Stock, Elements of X-ray Diffraction, Prentice Hall, New Jersey, 2001, 167-171.